

MHD ACCELERATION IN THE UNSTEADY EXPANSION OF A SHOCK TUBE DRIVER

By J. D. CASHMAN*

[Manuscript received 10 September 1971]

Abstract

The isentropic unsteady expansion of the driver gas in a shock tube is made to pass through an MHD interaction. The interaction is tailored so as to produce a new isentropic unsteady expansion downstream with greater energy than the original, which will drive a new shock of greater but constant velocity. Illustrative examples are calculated.

I. INTRODUCTION

Much effort in recent years has been directed towards increasing the shock speed in high speed shock tubes. One of the problems is that the energy lost in radiation sets a limit to the improvement that can be achieved by increasing the energy in the driver gas before the diaphragm bursts. An example of a device which overcomes this problem is the MAARC shock tube (Schneiderman *et al.* 1967), in which energy is added downstream from the diaphragm at effectively constant temperature. Other designs have been surveyed by Leonard and Rose (1968) who consider a range of two-stage devices. In these the first stage is some source of high energy gas, such as a shock tube or arc chamber, and the high energy gas expands steadily from a nozzle through the second stage in a magnetohydrodynamic (MHD) interaction. Conditions at the exit of the interaction are matched to those behind the shock by an isentropic expansion fan or, in some cases, an upstream propagating shock. Improvements in such arrangements are to be expected if the gas from the first stage expands unsteadily before it enters the second stage. There are two reasons for this:

- (1) energy added to the expanded gas should have greater effect than if added to the denser unexpanded gas, and
- (2) the expanded gas will be cooler so that radiation losses should be reduced.

In this paper a technique is proposed for adding energy well downstream from the sonic point in the unsteady expansion. Figure 1 shows the important parts of the proposed apparatus, with an $x-t$ diagram giving the shock trajectories, characteristics, and particle paths. The diaphragm separates a high pressure region on the left from a low pressure region on the right. There is a short MHD accelerator in the low pressure tube at a distance x_0 from the diaphragm.

The $x-t$ wave diagram in Figure 1 shows the behaviour after the diaphragm bursts. An initial shock S_1 propagates into region 1, the undisturbed low pressure gas, carrying behind it shock-heated gas into region 2. Behind a contact surface is an unsteady isentropic expansion in the driver gas, region 3. The high pressure region, as yet undisturbed by the expansion, is region 4. The initial shock is allowed to pass through the interaction and power is applied as the contact surface passes. The gas

* Faculty of Military Studies, University of New South Wales, Royal Military College, Duntroon, A.C.T. 2600.

leaving the interaction becomes the expansion $3'$ which will give rise to the secondary shock S_s and the expansion $3''$. In some cases, instead of the expansion $3''$ there may be an upstream-facing shock. It would be swept downstream in the moving gas. It will be assumed here that no such shock occurs, and conditions for its avoidance will be discussed in Section VII.

The shock S_s will overtake the initial shock S_i and accelerate it. There will follow a series of reflections back and forth between the contact surface and the main shock front. After the reflections have died out the main shock will have reached its final condition as S_f . The transition from S_i to S_f will be examined in Section V.

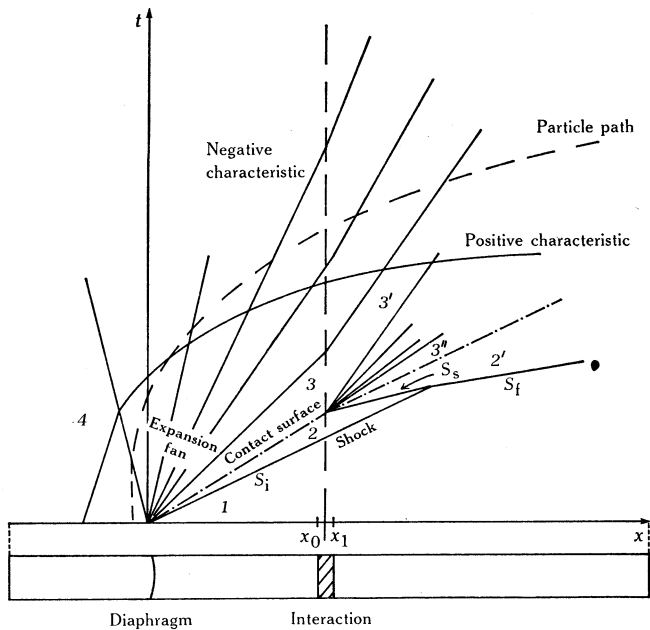


Fig. 1.—Shock tube containing the MHD interaction and the corresponding $x-t$ diagram showing the effects of the interaction on the characteristics, particle path, and shock front.

As the upstream unsteady expansion 3 flows through, the interaction is controlled in such a way as to create a downstream expansion $3'$ which will hold the final shock velocity constant. One method by which this may be achieved is to vary the electric and magnetic fields in the interaction so that the expansion $3'$ is a simple wave, similar to 3 upstream but of higher energy.

The main concern of this paper is to specify the interaction which will convert the isentropic simple wave in region 3 into another isentropic simple wave in region $3'$. The present work also gives a method for calculating the expected new shock speed and considers the interaction which will accelerate the main shock front most effectively. The paper is a theoretical examination of the proposed technique. Sections II, III, and IV develop the general specifications that the MHD interaction must meet and relate these to an interaction with crossed-field geometry, while Section V indicates

how the final shock speed may be determined. Section VI presents a calculated example to illustrate the techniques developed in the preceding sections. Section VII examines an optimum proportion between the current density and the magnetic field in the crossed-field interaction and relates this to the thermodynamic model used in Section VI. Finally, Section VIII draws some general conclusions about the accuracy and limits of the technique.

II. FORMATION OF SHOCK

Velocity and pressure are continuous across the contact surface between the driver gas (region 3 in Fig. 1) and the shock-heated gas (region 2). Thus the gas velocity behind the shock may be determined from the intersection of the pressure-velocity relations in the two gases.

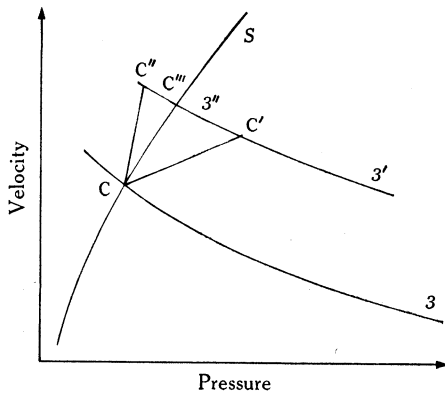


Fig. 2.—Shock and expansion curves. Curve S is the pressure-velocity relation in the gas behind the shock, while curves 3 and $3'$ are relations in the expansions upstream and downstream respectively from the interaction. The lines CC' , CC'' , and CC''' are possible paths taken by the gas particles in the interaction.

(a) Shock Curve

The pressure and velocity in the gas behind a shock propagating into a given gas take different values for different shock speeds. Their locus in the pressure-velocity plane will be referred to as a "shock curve". The relation between them may be written in the form

$$v = f_s(P), \quad (1)$$

where v and P are the velocity and pressure of the gas behind the shock. Let the shock curve S in Figure 2 represent this relation for the shock propagating into region 1 in Figure 1. The gas conditions behind the shocks S_1 and S_f both lie on this shock curve.

(b) Expansion Curve

In the expansion 3 in Figure 1, along positive characteristics defined by $dx/dt = v + a$, where a is the velocity of sound, changes in pressure and velocity are related by (Courant and Friedrichs 1948)

$$dv = -(a\rho)^{-1} dP. \quad (2a)$$

Along negative characteristics ($dx/dt = v - a$), they are related by

$$dv = (a\rho)^{-1} dP. \quad (2b)$$

As the positive characteristics pass from the expansion into the adjacent steady-flow region 4, the expansion is a simple wave. Gas properties are constant along negative characteristics, which are straight lines. The definition of the negative characteristics then becomes simply $x/t = v - a$, and this relates the gas properties to their position in the $x-t$ diagram.

As gas properties along negative characteristics are constant, all changes are related by equation (2a), which therefore represents a unique velocity-pressure relationship throughout the expansion. The converse is also true: if equation (2a) holds throughout the expansion, gas properties along negative characteristics are governed by both equations (2a) and (2b) and are therefore constant.

With an appropriate thermodynamic model, equation (2a) may be integrated to give the pressure-velocity relation in the expansion. The boundary conditions for this integration are those in region 4.

Let the curve 3 in Figure 2 represent this relation. It will be referred to here as the "expansion curve". Conditions at the contact surface will be given by the intersection of curves 3 and S at the point C . The following section considers alteration of the simple wave 3 in Figure 1 such that the expansion $3'$ is also a simple wave.

III. ALTERATION OF EXPANSION

(a) *Conditions for Constant Velocity Shock*

The MHD interaction is to be applied to the expansion so as to create conditions in which a new shock may emerge with higher velocity than the original. In order that the new velocity will be constant, the interaction will be made to vary so that the expansion created downstream ($3'$ in Fig. 1) will be a simple wave. Following the discussion in the previous section, for $3'$ to be a simple wave, two conditions must be met:

- (i) $3'$ must be isentropic, and
- (ii) equation (2a) must hold along all lines in its $x-t$ diagram.

(b) *"Short" Interaction*

Much simplification of the mathematics results from the assumption that the length of the interaction region Δx is short enough that the following two conditions are met:

(1) The interaction may be treated as a quasi-steady process with slowly varying input conditions. Thus, in the time during which a gas particle from region 3 of Figure 1 passes through the interaction, gas conditions at the entrance change by only a negligible fraction. If this time of passage is Δt , or approximately $\Delta x/v$, the condition becomes that for any gas property ζ

$$(\partial\zeta/\partial t)_{x=x_0} \Delta x/v \ll \zeta.$$

This condition depends on the position x_0 of the interaction. As $(\partial\zeta/\partial t)_{x=x_0}$ in the expansion becomes smaller without limit as x_0 increases, the condition may be met by positioning the interaction sufficiently far downstream from the diaphragm.

(2) It is an acceptable approximation to write

$$\Delta\zeta = [d\zeta/dx]_{\text{MHD}} \Delta x,$$

where $\Delta\zeta$ is the change from x_0 to x_1 of ζ and $[d\zeta/dx]_{\text{MHD}}$ is its rate of change in the interaction. This is a linear approximation to a nonlinear process and will normally be valid only while $\Delta\zeta$ is a small fraction of ζ .

We will now examine the short interaction which produces a downstream expansion satisfying conditions (i) and (ii) in subsection (a) above.

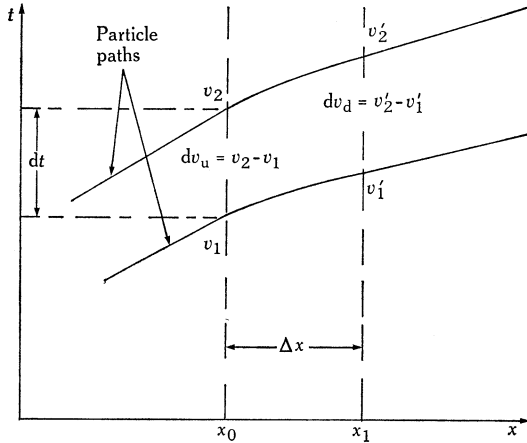


Fig. 3.— $x-t$ diagram of two particle paths through the MHD interaction. The x scale is greatly expanded by comparison with that of Figure 1. The velocities v'_1 and v'_2 are given by

$$v'_1 = v_1 + [dv_1/dx]_{\text{MHD}} \Delta x,$$

$$v'_2 = v_2 + [dv_2/dx]_{\text{MHD}} \Delta x.$$

Condition (i)

This condition is met by making constant the addition of entropy to unit mass of the gas in the interaction. Whence, the interaction must be such that

$$[ds/dx]_{\text{MHD}} = \text{constant}, \tag{3}$$

where s is the entropy per unit mass.

Condition (ii)

In the downstream expansion $3'$, equation (2a) holds along all lines in the family of positive characteristics. If it is made to hold along any line intersecting this family, it will be true along all lines in the expansion. It will be convenient to make equation (2a) hold along the line $x = x_1$ at the exit of the interaction.

In the $x-t$ diagram expanded around the interaction (Fig. 3), particle velocities on the two close particle paths differ by amounts dv_u upstream and dv_d downstream. The change in the velocity difference dv_u due to passage through the interaction may be expressed as

$$\Delta(dv) = dv_d - dv_u = \left(\left[\frac{dv_2}{dx} \right]_{\text{MHD}} - \left[\frac{dv_1}{dx} \right]_{\text{MHD}} \right) \Delta x$$

$$= \left(\frac{\partial}{\partial t} \left[\frac{dv}{dx} \right]_{\text{MHD}} \right)_{x=x_0} dt \Delta x. \tag{4}$$

In this equation the term expressed as a partial differential is the time rate of change

of $[dv/dx]_{\text{MHD}}$ as the electromagnetic parameters change in the interaction and as the properties of the gas change along the line $x = x_0$ in Figure 3. Similar expressions below have parallel interpretations. Thus the effect of the interaction on a small density difference $d\rho_u$ upstream may be expressed as

$$\Delta(d\rho) = \left(\frac{\partial}{\partial t} \left[\frac{d\rho}{dx} \right]_{\text{MHD}} \right)_{x=x_0} dt \Delta x. \quad (5)$$

Under the assumption of a quasi-steady process, conservation of mass provides that

$$\frac{d}{dx} \left[\rho v \right]_{\text{MHD}} = 0. \quad (6)$$

Equations (5) and (6) then give

$$\Delta(d\rho) = \frac{\rho}{v} \left\{ - \left(\frac{\partial}{\partial t} \left[\frac{dv}{dx} \right]_{\text{MHD}} \right)_{x=x_0} + \left[\frac{dv}{dx} \right]_{\text{MHD}} \left(- \frac{1}{\rho} \frac{\partial \rho}{\partial t} + \frac{1}{v} \frac{\partial v}{\partial t} \right)_{x=x_0} \right\} dt \Delta x. \quad (7)$$

Equation (2a) applies along all lines in the upstream expansion and therefore

$$\left(\frac{\partial \rho}{\partial t} \right)_{x=x_0} = - \frac{\rho}{a} \left(\frac{\partial v}{\partial t} \right)_{x=x_0}.$$

Including this in equation (7) then gives

$$\Delta(d\rho) = \frac{\rho}{v} \left\{ - \left(\frac{\partial}{\partial t} \left[\frac{dv}{dx} \right]_{\text{MHD}} \right)_{x=x_0} + \left[\frac{dv}{dx} \right]_{\text{MHD}} \frac{M+1}{v} \left(\frac{\partial v}{\partial t} \right)_{x=x_0} \right\} dt \Delta x, \quad (8)$$

where $M = v/a$ is the Mach number.

Condition (ii) requires that equation (2a) apply along the line $x = x_1$, that is,

$$dv_a + (a/\rho)d\rho_a = 0. \quad (9)$$

The left-hand side of this equation may be expanded to give

$$dv_u + \Delta(dv) + (a/\rho)d\rho_u + \Delta\{(a/\rho)d\rho\} = 0.$$

Noting that the first and third terms on the left-hand side sum to zero according to equation (2a) and expanding the fourth term gives

$$\Delta(dv) + d\rho_u \left(\frac{1}{\rho} \left[\frac{da}{dx} \right]_{\text{MHD}} - \frac{a}{\rho^2} \left[\frac{d\rho}{dx} \right]_{\text{MHD}} \right) \Delta x + \frac{a}{\rho} \Delta(d\rho) = 0. \quad (10)$$

$\Delta(dv)$ and $\Delta(d\rho)$ may be replaced according to equations (4) and (8). From equation (2a), the density change $d\rho_u$ in the expansion may be replaced by $-(\rho/a)dv_u$, or $-(\rho/a)(\partial v/\partial t)_{x=x_0} dt$. The quantity $[d\rho/dx]_{\text{MHD}}$ is the density rate of change in the interaction, and from equation (6) may be replaced by $-(\rho/v)[dv/dx]_{\text{MHD}}$. With these substitutions, and use of the definition of M , equation (10) becomes

$$\left\{ \frac{M-1}{M} \left(\frac{\partial}{\partial t} \left[\frac{dv}{dx} \right]_{\text{MHD}} \right)_{x=x_0} - \left(\frac{\partial v}{\partial t} \right)_{x=x_0} \frac{1}{a} \left(\left[\frac{da}{dx} \right]_{\text{MHD}} - \frac{1}{M^2} \left[\frac{dv}{dx} \right]_{\text{MHD}} \right) \right\} dt \Delta x = 0.$$

Dividing through by $\{(M-1)/M\}(\partial v/\partial t)_{x=x_0} dt \Delta x$ and rearranging gives

$$\left(\frac{\partial}{\partial v} \left[\frac{dv}{dx} \right]_{\text{MHD}}\right)_{x=x_0} = \frac{M}{M-1} \frac{1}{a} \left(\left[\frac{da}{dx} \right]_{\text{MHD}} - \frac{1}{M^2} \left[\frac{dv}{dx} \right]_{\text{MHD}} \right). \quad (11)$$

If the interaction is varied to make this equation true then the second condition (ii) will be satisfied.

We now have that an interaction constrained by equations (3) and (11) will cause the downstream expansion to be a simple wave. Up to this point no reference has been made to a specific interaction geometry. We will now examine one such geometry.

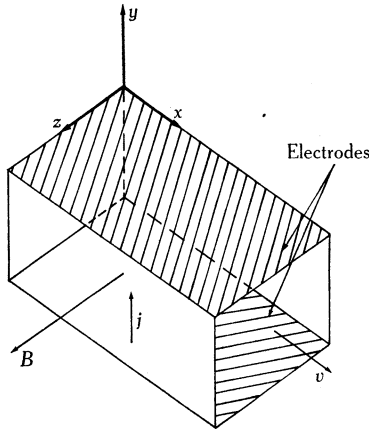


Fig. 4.—Geometry of crossed-field MHD interaction showing the directions of the magnetic field B , current density j , and flow velocity v .

IV. CROSSED-FIELD INTERACTION

The MHD interaction which will be considered here is of the crossed-field type illustrated in Figure 4. The top and bottom walls of the channel are electrodes between which a current density j exists. A magnetic field B is applied in the z direction. The effect of a Hall current, which may exist in the x direction, is the same as that of a reduced conductivity (Sutton and Sherman 1965, p. 394) and need not be considered here.

The assumptions are made that: the ratio of the channel length to width is large and end effects are negligible; the transverse pressure differences across the channel are small; and the magnetic Reynolds number $R_m = \mu\sigma v\delta$, where σ is the conductivity and δ a typical dimension, is considerably smaller than unity. In Appendix I an electrode geometry is described for which the appropriate value of δ is half the channel width and, for this geometry, the transverse pressure differences and end effects are assessed.

The equations governing the MHD interaction are

$$[d(\rho v)/dx]_{\text{MHD}} = 0, \quad (12a)$$

$$\rho v [dv/dx]_{\text{MHD}} = -[dP/dx]_{\text{MHD}} + jB, \quad (12b)$$

$$\rho v [d(\frac{1}{2}v^2 + h)/dx]_{\text{MHD}} = j^2/\sigma + vjB, \quad (12c)$$

where h is the enthalpy per unit mass.

Condition (i)

Equations (12b) and (12c) together with the exact differential

$$Tds = dh - \rho^{-1} dP,$$

where T is the temperature, give

$$[ds/dx]_{\text{MHD}} = j^2/\sigma T v \rho,$$

and the requirement presented by equation (3) is met by causing j to vary as

$$j = C(\sigma T v \rho)^{\frac{1}{2}}, \quad (13)$$

where C is a constant. σ is a property of the state of the gas and therefore the quantity $\sigma T v \rho$ at a position x may be calculated as a function of time, as described in Section II. Thus when a value of C and a position x_0 of the interaction are chosen, equation (13) determines j as a function of t .

Condition (ii)

The quantity $[dv/dx]_{\text{MHD}}$ is a function of B, j, v , and the thermodynamic state of the gas. In a given expansion, all the thermodynamic properties are related to v through the integration of equation (2a), and with equation (13) j is also. In a given expansion therefore, $[dv/dx]_{\text{MHD}}$ may be considered to be a function of B and v . In this case the left-hand side of equation (11) may be written

$$\left(\frac{\partial}{\partial B} \left[\frac{dv}{dx} \right]_{\text{MHD}} \right)_{v=\text{const}} \frac{dB}{dv} + \left(\frac{\partial}{\partial v} \left[\frac{dv}{dx} \right]_{\text{MHD}} \right)_{B=\text{const}}.$$

Setting this expression equal to the right-hand side of (11) and rearranging gives

$$\frac{dB}{dv} = \frac{\frac{M}{M-1} \frac{1}{a} \left(\left[\frac{da}{dx} \right]_{\text{MHD}} - \frac{1}{M^2} \left[\frac{dv}{dx} \right]_{\text{MHD}} \right) - \left(\frac{\partial}{\partial v} \left[\frac{dv}{dx} \right]_{\text{MHD}} \right)_{B=\text{const}}}{\left(\frac{\partial}{\partial B} \left[\frac{dv}{dx} \right]_{\text{MHD}} \right)_{v=\text{const}}}. \quad (14)$$

This equation may be integrated to give the variation of B with v if expressions for $[da/dx]_{\text{MHD}}$ and $[dv/dx]_{\text{MHD}}$ are available. Such expressions result from solving equations (12) with a thermodynamic model of the gas, as is illustrated in the numerical example in Section VI. Since integration of equation (14) gives B as a function of v , and gas of velocity v arrives at the entrance x_0 to the interaction at a time $t = x_0/(v-a)$ given by the equation for the negative characteristics, B may be determined as a function of t .

V. FINAL SHOCK SPEED

When the time variation of j and B have been determined, the time variation of the gas properties at the exit of the interaction may be calculated. The pressure at the exit of the short interaction will be given by $P + [dP/dx]_{\text{MHD}} \Delta x$, where P is the pressure at the entrance. A similar expression will yield the exit velocity. When these are plotted against one another, a curve such as 3' in Figure 2 results. This is the relation along

the line $x = x_1$ in Figure 3 but, following the discussion in Section III, it applies throughout the expansion.

When the interaction starts, the secondary shock S_s propagates forward to overtake the initial shock S_i (see Fig. 1) and accelerate it. At the same time a wave propagates into the gas upstream of the contact surface. This may be either the expansion $3''$ or a shock wave, depending on the type of interaction. When the secondary shock overtakes and accelerates the initial shock, a reflection wave travels back towards the contact surface. Once this reflection meets the contact surface, in general a wave will be transmitted beyond into the region $3'$ and a wave will be reflected back towards the main shock front. The final state will be the result of a series of reflections back and forth between the main shock front and the contact surface, together with a series of waves, which may be either rarefactions or compressions, transmitted into the expansion $3'$. The length of the shock tube downstream from the interaction must be great enough for these reflections to become negligible.

As the short interaction does not alter the properties of the gas passing through it by more than a small fraction, the shock and expansion waves caused by it will be weak. Any expansion waves transmitted into the region $3'$ upstream from the contact surface will expand it further but will not alter its simple wave character; any weak shocks will affect the simple wave character only slightly. It may be expected that the strongest of the transmitted shocks, if any, would be the first to appear. This was suggested in Section I as an alternative to $3''$, and a technique for its avoidance is described in Section VII. Thus it is assumed that the final pressure-velocity relationship in the region $3'$ is unaffected by these transmitted waves, and is given by the curve $3'$ in Figure 2.

After the final shock is established, gas pressure and velocity are continuous between region $3'$ and the main shock front, and their values immediately behind the shock are given by the intersection of curves $3'$ and S in Figure 2. The velocity of the shock is related to the conditions behind it in a way which depends on the thermodynamic nature of the gas, and this relation is derived for a perfect gas in appropriate texts (see e.g. Courant and Friedrichs 1948). Another relation is suggested in the next section when the gas is singly ionizing.

VI. CALCULATED EXAMPLE

To illustrate the techniques described in the previous sections, we consider the following numerical example. Both the driver gas and the gas into which the shock propagates are argon, which is taken to be a monatomic singly ionizing gas whose ionization fraction is governed by the Saha equation. In Figure 1, region 1 is assumed to contain gas at a pressure of 105 N m^{-2} (0.8 mmHg) and a temperature of 300 K . Region 4 contains gas at a pressure of $4.5 \times 10^6 \text{ N m}^{-2}$ ($\sim 45 \text{ atm}$) and a temperature of 19400 K .

Appendix II gives details of the calculation of the shock and expansion curves. These are plotted as the curves S and 3 in Figure 5. The speed of the gas behind the shock is 8500 m s^{-1} . On the assumption used in Appendix II that the density ratio across the shock is high, this value closely approximates the shock speed.

(a) Determination of j and B

As gas properties are constant along straight lines radiating from the origin in Figure 1, the time scale of events in the interaction is proportional to the distance x_0 . The quantities j and B are therefore determined as functions of the parameter $\tau = t/x_0$, the time per unit distance of the interaction downstream from the diaphragm.

The assumed interaction length Δx is 1 m. However, it is evident from equations (12b) and (12c) that if the x scale is changed by a factor F say, and j and B are each scaled by $F^{-\frac{1}{2}}$, the results of the interaction will be unaffected. Thus the values of j and B presented in Figure 6 below are plotted as $j(\Delta x)^{\frac{1}{2}}$ and $B(\Delta x)^{\frac{1}{2}}$.

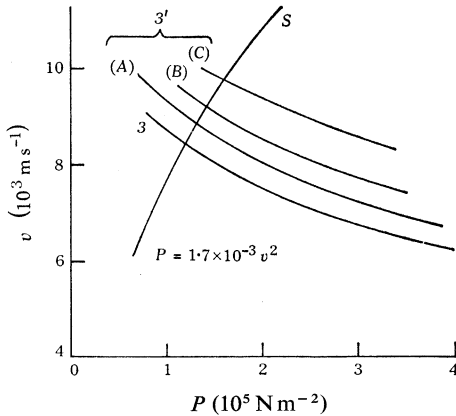


Fig. 5.—Shock and expansion curves for the conditions described in Section VI. The curves $3'(A)$, $3'(B)$, and $3'(C)$ are expansions created by passing expansion 3 through three different interactions.

The required current density is given by equation (13). Apart from the arbitrary constant C , the right-hand side may be calculated as a function of τ . Three curves of j versus τ , corresponding to three different values of C , are plotted in Figure 6.

In the calculation of the conductivity σ the method of Lin *et al.* (1955) has been used. The result is a slowly varying quantity of magnitude approximately 10^4 mho m^{-1} . The effect of a Hall current has been neglected for simplicity. The magnitude of this effect may be assessed as follows. Since σ is approximately related to the average collision frequency ν between electrons and ions or atoms by (Sutton and Sherman 1965, p. 154) $\sigma = n_e e^2 / m_e \nu$ (n_e , e , and m_e being the electron number density, charge, and mass respectively) while the cyclotron frequency ω of the electrons in a magnetic field is eB/m_e , the Hall parameter ω/ν is therefore given by $B\sigma/en_e$. The number density n_e may be calculated from the value of the ionization fraction α . In the present example the largest value taken by α is 0.7, giving rise to an effective conductivity reduction by a factor of 1.5.

The time variation of the magnetic field B requires integration of equation (14). Details of this integration for the present case are given in Appendix III. To each of the current density curves in Figure 6 there corresponds a family of magnetic field curves resulting from variation of the arbitrary initial value B_0 . One magnetic field curve is plotted in each case, and the values of B_0 are indicated on the graphs.

In Appendix I it is shown that, with the electrode geometry described there, the magnetic Reynolds number R_m is given by equation (A1). If a duct width of 1 cm is chosen then, with a conductivity of 10^4 mho m^{-1} and a contact surface velocity of

8500 m s⁻¹, $R_m = 0.53$. A lower value than this would be desirable, but it may be noted that this is the worst case; following the contact surface, the velocity decreases and R_m with it. As is argued in Appendix I, the more important considerations are the transverse pressure differences and the end effects. The former differences may be ignored so long as the inequality (A2) is observed. At the contact surface the pressure is 1.6×10^5 N m⁻² and (A2) gives, with $W = 1$ cm,

$$j^2 \ll 10^{16} \text{ A}^2 \text{ m}^{-4}.$$

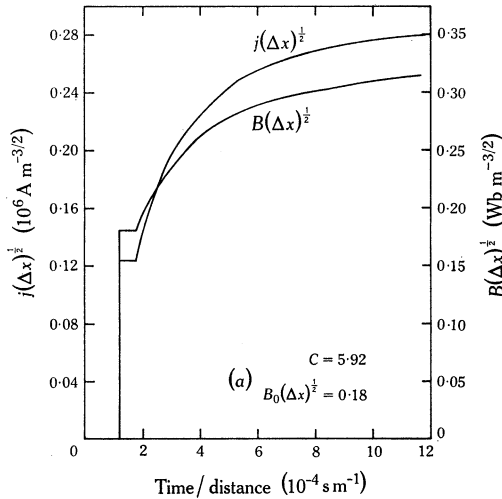
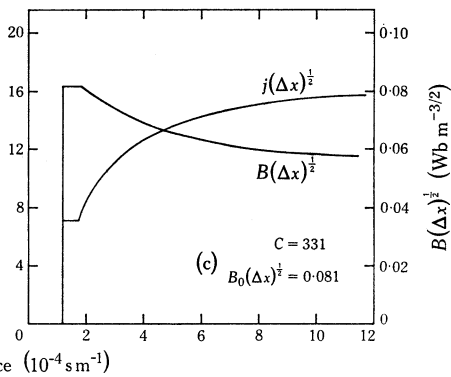
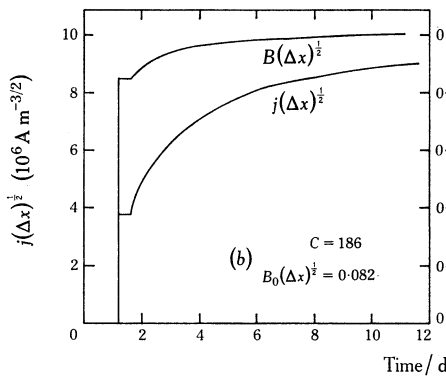


Fig. 6.—Variations of $j(\Delta x)^{\frac{1}{2}}$ and $B(\Delta x)^{\frac{1}{2}}$ for the conversion of the expansion 3 in Figure 5 into the expansions:

- (a) curve 3'(A),
- (b) curve 3'(B),
- (c) curve 3'(C).

The corresponding values of the constant C (expressed in units of $J^{\frac{1}{2}} \text{ kg}^{-\frac{1}{2}} \text{ m}^{-\frac{1}{2}} \text{ K}^{-\frac{1}{2}}$) in equation (13) and the initial value $B_0(\Delta x)^{\frac{1}{2}}$ (in $\text{Wb m}^{-3/2}$) of $B(\Delta x)^{\frac{1}{2}}$ applied as the contact surface passes are indicated in each case.



Following the contact surface j increases, but P increases also and this constraint becomes less severe. It is also shown in Appendix I that the end effects are unimportant provided the inequality (A4a) is observed. The gas at the contact surface has a density of 4.3×10^{-2} kg m⁻³, and (A4a) becomes approximately

$$j^2 \ll 2 \times 10^{16} \text{ A}^2 \text{ m}^{-4}.$$

Following the contact surface ρ increases faster than v decreases so that their product increases, and this constraint also becomes less severe.

On the above analysis the transverse pressure differences impose the lower limit on j . The current densities given in Figure 6 taking $\Delta x = 1$ m all fall below this limit. The worst case is that of Figure 6(c), where the current density at the contact surface gives $j^2 = 5.6 \times 10^{13} \text{ A}^2 \text{ m}^{-4}$, well within the limit of $10^{16} \text{ A}^2 \text{ m}^{-4}$.

The allowable limit on B is given by equation (A4b). At the contact surface this becomes approximately $B^2 \ll 0.9 \text{ Wb}^2 \text{ m}^{-4}$. Following the contact surface the product ρv in the right-hand side of (A4b) increases, and this constraint becomes less severe. The values of B given in Figure 6 all fall within this limit at the contact surface. The worst case is that of Figure 6(a), where the field at the contact surface gives $B^2 = 0.032 \text{ Wb}^2 \text{ m}^{-4}$.

(b) Final Shock Speeds

When j and B are known as functions of time, the velocity and pressure of the gas at the exit may be calculated as functions of time and hence of one another. In Figure 5, curve $3'(A)$ is the pressure-velocity relation in the expansion created by the interaction whose j and B curves are given in Figure 6(a). Conditions behind the final shock are given by the intersection of curves $3'(A)$ and S . The gas behind the shock has a velocity of 8900 m s^{-1} . The shock velocity is approximately equal to the gas velocity and has increased by 400 m s^{-1} from its initial value.

In Figure 6(b) the current density is greater and the magnetic field is slightly weaker than before. The expansion at the exit of this interaction is plotted as curve $3'(B)$ in Figure 5. This interaction increases the shock speed to 9200 m s^{-1} .

Figure 6(c) shows an interaction in which both pressure and velocity have increased by about 25%. They are plotted as curve $3'(C)$ in Figure 5. The shock velocity has increased by 1300 m s^{-1} . In this example, the assumption of a short interaction as described in Section III may be unreliable, since the changes in gas properties in the interaction are no longer small fractions of their values at the entrance.

VII. OPTIMUM PROPORTIONS FOR CURRENT DENSITY AND MAGNETIC FIELD

The arbitrary constants which occur in the calculations of j and B allow control of the relative magnitudes of these parameters. In this section we seek a criterion for the optimum proportion between them.

In Figure 2 the gas conditions at the contact surface upstream from the interaction are given by the point C. The driver gas at the contact surface passes through the interaction along a line of slope $[dv/dP]_{\text{MHD}}$ to a point on the curve $3'$. The lines CC' , CC'' , and CC''' indicate possible paths. The interaction along CC' produces a gas at the exit of higher pressure and lower velocity than is compatible with conditions at the contact surface (which must lie on the shock curve). Consequently the expansion $3'$ must expand further until the shock conditions are reached. The expansion $3''$ achieves this. The interaction along CC'' , however, produces a gas whose pressure is too low and velocity too high to be compatible with conditions at the contact surface. Consequently the expansion $3'$ must be re-compressed and a shock will propagate upstream with coordinates in which the contact surface is stationary. Schneiderman *et al.* (1967) have discussed the possibility of a backwards propagating shock downstream from the MAARC accelerator. Thus, whether the wave propagating into region

3' is an expansion like 3" in Figure 1 or a shock depends on whether the slope of the interaction path in Figure 2 is less than or greater than the slope of the shock curve.

If the upstream propagating shock is to be avoided, the slope of the interaction must be less than that of the shock curve. This may be expressed as

$$[dv/dP]_{\text{MHD}} \leq [dv/dP]_{\text{sh}}, \quad (15)$$

where $[dv/dP]_{\text{sh}}$ is the slope of the shock curve. It may be expected that the most accurate construction of the new simple wave will result when the proportional increments in pressure and velocity are approximately equal, or

$$[dv/dP]_{\text{MHD}} \approx v/P. \quad (16)$$

The optimum interaction is that in which equation (16) holds as closely as is consistent with equation (15).

For the thermodynamic model employed in Section VI, the shock curve is parabolic (Appendix I) and the condition (15) becomes

$$[dv/dP]_{\text{MHD}} \leq v/2P. \quad (17)$$

Equation (16) will most closely be met if (17) is written as an equality. Using the relations presented in Appendix III for the crossed-field interaction, this gives the relation between the current density and magnetic field of

$$j = \varepsilon^{-1} \{ (2 + \gamma^*) / (2 + \gamma^* M^2) \} \sigma v B. \quad (18)$$

There are two freedoms in the determination of j and B , resulting from the two arbitrary constants. Application of equation (18) at the contact surface removes one of these freedoms. Exercise of the remaining freedom gives control of the strength of the interaction and hence of the magnitude of the shock acceleration.

VIII. CONCLUSIONS

A technique has been described for creating a simple wave expansion downstream of an MHD interaction in a shock tube and thereby accelerating the shock. The accuracy with which the downstream expansion resembles a simple wave depends on the accuracy with which the specified current density and magnetic field can be reproduced. In many cases these quantities will be produced by discharging capacitor banks and will meet their specifications only approximately over a limited period. The reconstructed expansion will be an imperfect replica of the ideal and the final shock velocity will not be exactly constant. Other effects, such as transverse pressure differences, end effects, viscosity, and radiation will introduce further departures from ideal behaviour.

The assumption has been made in this paper that the interaction is short enough to be treated as a linear process. Strict compliance with this restriction may be relaxed somewhat as the inaccuracy thereby introduced may be less than that due to the effects suggested above. The final shock velocity will be increased but will become less constant. The limit at which this defect becomes unacceptable will be determined by trial, and the application to which the shock-induced flow is to be put, but one may perhaps hope for a velocity increase of up to 100%.

If the velocity of the final shock must be maintained within closer limits, a number of short interactions could be used in series. This may be preferable to the alternative of a single long interaction, for then the differential equations which describe the flow through the interaction would require integration. In addition it may no longer be valid to regard the integration as a quasi-steady process and the implications of this would require examination.

IX. ACKNOWLEDGMENT

This work is based on an M.Sc. thesis presented to the Australian National University. It was supervised by Dr. R. J. Stalker, to whom the author is grateful for much advice and critical discussion.

X. REFERENCES

- CASHMAN, J. D. (1971).—*Aust. J. Phys.* **24**, 847.
 COURANT, R., and FRIEDRICHS, K. O. (1948).—“Supersonic Flow and Shock Waves.” (Interscience: New York.)
 JOHNSON, M. R. (1967).—*Physics Fluids* **10**, 539.
 KANTROWITZ, A. (1957).—In “Magnetohydrodynamics.” (Ed. R. K. M. Landshoff.) (Stanford Univ. Press.)
 LEONARD, R. L., and ROSE, P. H. (1968).—*AIAA JI* **6**, 448.
 LIN, SHAO-CHI, RESLER, E. L., and KANTROWITZ, A. (1952).—*J. appl. Phys.* **23**, 1390.
 LIN, SHAO-CHI, RESLER, E. L., and KANTROWITZ, A. (1955).—*J. appl. Phys.* **26**, 95.
 SCHNEIDERMAN, A. M., PUGH, E. R., and PATRICK, R. M. (1967).—Avco—Everett Res. Rep. No. 263.
 SHERCLIFF, J. A. (1965).—“A Textbook of Magnetohydrodynamics.” (Pergamon Press: Oxford.)
 SUTTON, G. W., and SHERMAN, A. (1965).—“Engineering Magnetohydrodynamics.” (McGraw-Hill: New York.)

APPENDIX I

Electrode Geometry

Figure 7 shows an electrode geometry in which the return current flows in the negative y direction down the outside of the duct wall. This arrangement (Shercliff 1965) confines the magnetic field B_i induced by the current to the x direction only, except at the ends. In the body of the field then the Maxwell equation $\text{curl } \mathbf{B} = \mu \mathbf{j}$ becomes $\partial B_i / \partial z = \mu j$. The induced field B_i is zero at the centre of the duct and reaches a maximum value of $\frac{1}{2} \mu j W$ at the edge, W being the duct width. If the electrodes are short-circuited, the current density is $j = \sigma v B$ and the ratio of the maximum value of the induced field to the applied field is given by

$$R_m = \frac{1}{2} \mu \sigma v W, \quad (\text{A1})$$

the magnetic Reynolds number based on the half-width of the duct. It is necessary to specify the electrode geometry in this way since in many realistic cases the value of R_m based on the interaction length is not less than unity.

The induced field has two effects which may be deleterious: the longitudinal component inside the interaction may give rise to large pressure differences across the

duct, and the transverse component at the entrance to the interaction may cause current eddies in the gas as it enters, possibly causing a shock to be reflected upstream from the entrance. Provided these two effects are not serious, the value of R_m is relatively unimportant. Criteria for assessing these effects are now developed.

The longitudinal induced field gives rise to a transverse pressure gradient $\partial P/\partial z = jB_i$. If j is uniform, $B_i = \mu jz$ and the pressure difference between the axis and the walls may be found by integration to be $\frac{1}{8}\mu j^2 W^2$. So long as this is a small fraction of the pressure of the gas entering the interaction, i.e.

$$j^2 \ll 8P/\mu W^2, \tag{A2}$$

the gas may be assumed unvarying in the transverse direction.

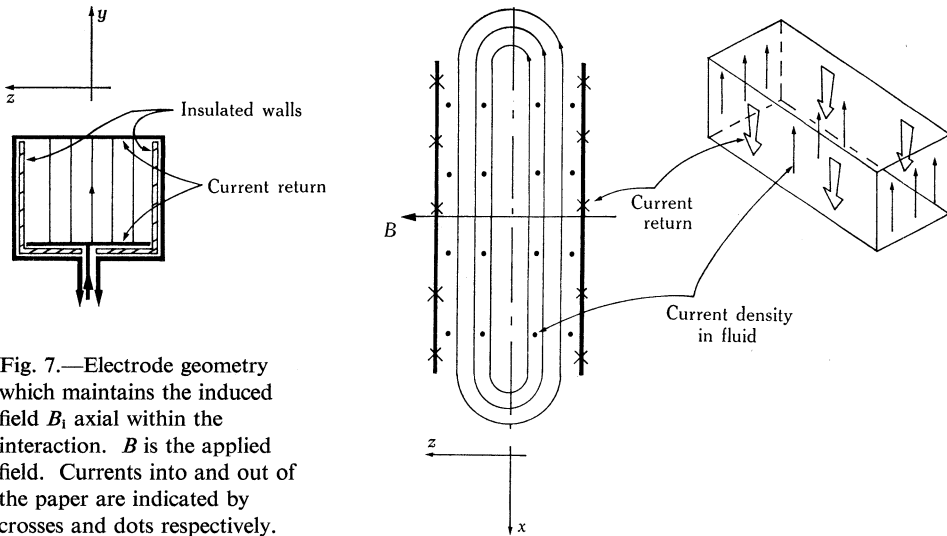


Fig. 7.—Electrode geometry which maintains the induced field B_i axial within the interaction. B is the applied field. Currents into and out of the paper are indicated by crosses and dots respectively.

The end effects are assessed in the following manner. Kantrowitz (1957) has described the entry of a shock wave into the field created by a solenoid wound around the duct. Currents are induced in the supersonic flow behind the shock, which therefore reduces in velocity. If unity Mach number is reached, the flow chokes and an upstream facing shock is formed. Although the geometry proposed here is different from that of Kantrowitz, the important requirement is evidently that the flow must not approach unity Mach number. Johnson (1967) has found an expression for the parameter $N = \sigma B^2 L/\rho v$ which causes a perfect gas flow to choke at the end of an interaction of length L . Applying his results to the case where the electrodes in Figure 7 are short-circuited, we find

$$N = \frac{1 - M_e^2}{2\gamma M_e^2} + \frac{\gamma + 1}{4\gamma} \ln\left(\frac{(\gamma + 1)M_e^2}{2 + (\gamma - 1)M_e^2}\right),$$

where γ is the ratio of the specific heats at constant pressure and constant density and M_e is the Mach number of the flow at the entrance. For a given γ , as M_e increases without bound N approaches a limiting value which is almost reached with $M_e = 3$.

For $\gamma = 5/3$, this limit is 0.26 and rises without bound as γ decreases towards unity. The ionized gases, which are the usual fluids in the present application, behave in some respects like perfect gases with low values of γ (Cashman 1971) and hence the value of N needed to choke the flow is greater than that for a perfect gas. Thus, if it is ensured that a perfect gas flow will not choke, it will be ensured *a fortiori* that the ionized flow will not choke.

It is assumed here that the eddy currents and their effects on the flow at the entrance to the interaction will be similar in magnitude to those which would occur between the short-circuited electrodes of Johnson's (1967) analysis. The actual eddy currents have a return path through the gas of higher resistance and so should be smaller than those between the shorted electrodes. Thus, avoidance of undesired end effects with shorted electrodes constitutes a more severe precaution than that required by the real situation. The magnetic field giving rise to eddy currents is due to the applied field B and the transverse component of the induced field B_i , both extending a distance comparable with the duct width W beyond the interaction. B_i has a transverse component whose order of magnitude is taken to be that of the axial field inside the duct, namely $\frac{1}{2}\mu jW$. In this case the effective value of N due to these end fields will be of order

$$N \approx \sigma W(B + \frac{1}{2}\mu jW)^2 / \rho v. \quad (\text{A3})$$

In a perfect gas flow with $\gamma = 5/3$ and $M_e \gtrsim 3$, the value $N = 0.26$ would cause choking. Thus N must be much less than 0.26 if the flow is to be essentially unperturbed by the end effects. For this to be so equation (A3) gives approximately

$$j^2 \ll \rho v / \mu^2 \sigma W^3 \quad \text{and} \quad B^2 \ll \rho v / 4\sigma W. \quad (\text{A4a, b})$$

It is apparent from equations (A1) to (A4) that the limitations imposed by the need for small R_m , small transverse pressure differences, and small end effects are all made less severe by reducing the channel width. The limitations set by the second and third factors may be further relieved by reducing j and B and increasing the channel length. It may be noted that increasing the length Δx does not violate the assumption of a short interaction provided the conditions (1) and (2) given in Section III(b) are satisfied.

APPENDIX II

Shock and Expansion Curves

Under the conditions described in Section VI the gases in the expansion and behind the shock are both ionized. The thermodynamic behaviour of singly ionized argon is described by the equation of state

$$P = 207.7 \rho(1 + \alpha)T$$

and the Saha equation

$$\alpha^2 / (1 - \alpha^2) = 0.4 P^{-1} T^{5/2} \exp(-18.2 \times 10^4 T^{-1}),$$

where α is the ratio of the number of ions to the number of ions and atoms. All quantities are in SI units.

Shock Curve

Conservation of mass, momentum, and energy across the shock gives the equations

$$\rho_1 v_s = \rho_2(v_s - v_2), \quad (\text{A5a})$$

$$P_1 + \rho_1 v_s^2 = P_2 + \rho_2(v_s - v_2)^2, \quad (\text{A5b})$$

$$h_1 + \frac{1}{2}v_s^2 = h_2 + \frac{1}{2}(v_s - v_2)^2, \quad (\text{A5c})$$

where v_s is the shock speed and the subscripts 1 and 2 refer to regions 1 and 2 in Figure 1. These equations have been solved numerically with the above thermodynamic relations for a range of cases (Lin *et al.* 1952) and it is found that the density ratio across ionizing shocks is much greater than that across non-ionizing shocks, where it has an upper limit of four. Assuming therefore $\rho_2 \gg \rho_1$, equations (A5a) and (A5b) yield the strong shock relation

$$P_2 = \rho_1 v_s^2.$$

Under the conditions described for region 1, $\rho_1 = 1.7 \times 10^{-3} \text{ kg m}^{-3}$, and this relation is plotted as the shock curve S in Figure 5.

Expansion Curve

The isentropic relation between T and α is given by (Cashman 1971)

$$\frac{T}{18 \cdot 2 \times 10^4} = \frac{1 + \alpha}{C_0 - \frac{5}{2}\alpha - 2 \ln\{\alpha/(1-\alpha)\}},$$

where C_0 is a constant. With the equation of state and the Saha equation, isentropic relations between all the thermodynamic variables may be determined. Then equation (2a) may be integrated numerically, using the boundary conditions of region 4 in Figure 1, to give the expansion curve 3 in Figure 5.

APPENDIX III

Integration of Equation (14)

The integration of equation (14) requires evaluation of the terms $[dv/dx]_{\text{MHD}}$ and $[da/dx]_{\text{MHD}}$. An expression for the first term may be found by solving equation (12) for singly ionizing argon to give (Cashman 1971)

$$\left[\frac{dv}{dx} \right]_{\text{MHD}} = \frac{1}{M^2 - 1} \frac{j(vB - \epsilon j/\sigma)}{P\gamma^*}, \quad (\text{A6})$$

where

$$\gamma^* = a^2 \rho / P \quad (\text{A7a})$$

$$= \frac{5\phi^2 + \alpha(1-\alpha)(\frac{5}{2}\phi + 1)^2}{3\phi^2 + \alpha(1-\alpha)\{(\frac{3}{2}\phi + 1)(\frac{5}{2}\phi + 1) - \phi\}} \quad (\text{A7b})$$

and

$$\epsilon = \frac{2\phi^2 + \alpha(1-\alpha)(\frac{5}{2}\phi + 1)\phi}{3\phi^2 + \alpha(1-\alpha)\{(\frac{3}{2}\phi + 1)(\frac{5}{2}\phi + 1) - \phi\}},$$

in which $\phi = T/18 \cdot 2 \times 10^4$.

An expression for $[da/dx]_{\text{MHD}}$ may be found as follows. Differentiating equation (A7a) and rearranging gives

$$\left[\frac{da}{dx}\right]_{\text{MHD}} = \frac{1}{2}a \left(\frac{1}{P} \left[\frac{dP}{dx}\right]_{\text{MHD}} - \frac{1}{\rho} \left[\frac{d\rho}{dx}\right]_{\text{MHD}} + \frac{1}{\gamma^*} \left[\frac{d\gamma^*}{dx}\right]_{\text{MHD}} \right). \quad (\text{A8})$$

From equations (12a) and (12b), $[d\rho/dx]_{\text{MHD}}$ and $[dP/dx]_{\text{MHD}}$ may be expressed in terms of $[dv/dx]_{\text{MHD}}$. Examination of the expression (A7b) for γ^* shows it to take values between 5/3 and 1 for the whole range of T and α . Thus the approximation is used here that γ^* is constant and $[d\gamma^*/dx]_{\text{MHD}}$ is set equal to zero. With these substitutions equation (A8) becomes

$$\left[\frac{da}{dx}\right]_{\text{MHD}} = \frac{1}{2}a \left((1 - \gamma^* M^2) \frac{1}{v} \left[\frac{dv}{dx}\right]_{\text{MHD}} + \frac{jB}{P} \right), \quad (\text{A9})$$

in which $[dv/dx]_{\text{MHD}}$ is given by equation (A6).

The term $(\partial[dv/dx]_{\text{MHD}}/\partial v)_{B=\text{const}}$ in the numerator on the right-hand side of equation (14) cannot easily be expressed in closed form, as most of the parameters of which $[dv/dx]_{\text{MHD}}$ is a function are related to v . However, it may be readily evaluated numerically for the expansion under consideration. The denominator term may be found from equation (A6) to be given by

$$\left(\frac{\partial}{\partial B} \left[\frac{dv}{dx}\right]_{\text{MHD}} \right)_{v=\text{const}} = \frac{jv}{(M^2 - 1)P\gamma^*}.$$

Thus the right-hand side of equation (14) may be integrated numerically to give the variation of B with v and hence with τ . This integration introduces an arbitrary initial value B_0 .